Q. J. R. Meteorol. Soc. (1995), **121**, pp. 1867–1889

An intercomparison of three vegetation/soil models for a sparse vineyard canopy

By B. J. J. M. van den HURK*, A. VERHOEF, A. R. van den BERG and H. A. R. de BRUIN
Wageningen Agricultural University, The Netherlands

(Received 23 November 1994; revised 31 March 1995)

SUMMARY

Three Soil–Vegetation–Atmosphere Transfer models simulating fluxes collected at a dry sparse vineyard site in La Mancha, Spain, are intercompared. The algorithms used to describe soil heat-flux density, aerodynamic transfer of water and heat between the surface and the atmosphere, and crop evaporation all have a different physical basis in these models. A common feature of the models is that interaction of many processes takes place via the surface temperature.

Large differences are found between the predicted soil heat-flux densities, caused by a poor physical description of heat storage in the soil and by the choices of soil coefficient values. Significant differences in the parametrization of the aerodynamic transfer between the surface and the atmosphere also exist, with a clear impact on predictions of surface temperature. Crop evaporation is underestimated by models taking the effect of soil moisture depletion or atmospheric humidity deficit on crop resistance into account.

A suggestion is made for an optimal choice of various model components to describe the observed fluxes best.

KEYWORDS: Land surface parametrizations Soil models Surface fluxes Vegetation models

1. INTRODUCTION

For large-scale models such as global circulation models (GCMs) the lower boundary condition is often provided by a Soil–Vegetation–Atmosphere Transfer (SVAT) model. As pointed out by Garratt (1992), the description of the exchange processes between the surface and the atmosphere is of great influence on the long-term predictions of these larger-scale models.

A wide range of SVAT models is in use nowadays, varying from models based on the simple big-leaf concept (Monteith 1965) to complicated dual-source models (Sellers *et al.* 1986). A considerable number of papers dedicated to the verification of one or more of these SVAT schemes for various land-surface types has appeared (e.g. Dolman and Wallace 1991; Viterbo and Beljaars 1995; and others).

Obviously, a SVAT model intended to provide the lower boundary condition in GCMs needs to be able to describe a wide range of surface types, varying from completely vegetated to sparcely vegetated or completely bare surfaces. Sparse-canopy surfaces exhibit rather demanding features with respect to the exchange of momentum, scalars and heat between the surface and the atmosphere.

For the aerodynamic exchange, a difference is made between the exchange of momentum and of scalars as heat, water vapour, carbon dioxide or trace gases. Surface-roughness elements acting as a momentum sink are usually parametrized by extrapolation of the wind profile to a hypothetical sink level at height $d + z_{0m}$, where d is the zero-plane displacement and z_{0m} the roughness length for momentum. Both parameters depend on the presence of roughness elements, characterized by the surface fraction being covered, and the spacing and height of the elements. Measurements and theoretical considerations reveal a difference between the exchange rates of scalars and momentum. The transport of water vapour, heat or trace gases is considered less efficient than momentum transport in most cases, owing to the absence of bluff-body forces for scalar exchange (Thom 1972; Beljaars and Holtslag 1991). Models treating the surface as a single homogeneous layer impose an 'excess' resistance for scalars to account for this effect. This is equiv-

* Corresponding author: KNMI PO Box 201, 3730 AE De Bilt, The Netherlands.

alent to adopting a different roughness length for scalars, z_{0h} (Garratt and Hicks 1973). Experimental quantification of this roughness length has been carried out for many surface types, particularly using radiometric surface-temperature measurements (Kustas *et al.* 1989; Menenti *et al.* 1989). For sparse canopies the interpretation of z_{0h} is far from straightforward. The heat exchange takes place at various levels, and the source distribution is determined by various environmental parameters, such as radiation, canopy evaporation, or forced convection. Two-layer models avoid the definition of a single source level by parametrizing the sensible- and latent-heat exchange at two separate levels: the canopy and the underlying substrate. The absence of bluff-body forces for scalar exchange is accounted for by additional resistances within the canopy layer. The turbulent exchange of sensible and latent heat between the canopy, the substrate and the air above are treated separately. Parametrization of these resistances is carried out by adopting assumptions about the turbulent exchange within the canopy layer and the effective sink level. This level can either be a fixed function of the canopy height (Shuttleworth and Wallace 1985), a more complex function of leaf-area index (LAI) (Choudhury and Monteith 1988), or crop density (Raupach 1992). However, turbulence characteristics within the canopy layer are rather complex and not easily defined using simple parameters (Van den Hurk and McNaughton 1995).

In a two-layer model, the resistances within the canopy layer provide an excess resistance equivalent to adopting $z_{0m}/z_{0h} > 1$. Blyth and Dolman (1995) used a two-layer model to explore the value of z_{0m}/z_{0h} for a sparse canopy. The apparent aerodynamic resistance for heat transfer, r_{ah}, was deduced from the simulated total sensible-heat-flux density H, the air temperature T_a, and a mean surface temperature T_{sur}, according to

$$r_{ah} = \rho c_p \frac{T_{sur} - T_a}{H} \tag{1}$$

where ρ denotes the air density and c_p the specific heat capacity of dry air. T_{sur} was obtained from a linear interpolation of the model predictions of canopy temperature T_l and ground temperature T_g:

$$T_{sur} = f_c T_l + (1 - f_c) T_g \tag{2}$$

where f_c is the surface fraction covered with vegetation. The value of z_{0h} is then obtained from

$$z_{0h} = \frac{z_a}{\exp\{r_{ah}\kappa u_* + \Psi_h(z_a/L)\}} \tag{3}$$

in which z_a is the reference level, κ the Kármán constant, u_* the friction velocity, L the Monin–Obukhov length and Ψ_h a stability correction. The resulting roughness length for heat appeared not as a function of the surface itself (as is the case for z_{0m}) but showed a clear variation with radiation, wind and even vapour-pressure deficit. Apparently, the variation of the distribution of the heat sources causes the variation of z_{0h}. Similar results were obtained experimentally by Kustas *et al.* (1989) and Verhoef *et al.* (1994, personal communication).

The second issue of interest for sparse-canopy surfaces is the treatment of the soil heat-flux density. Under conditions where a significant part of the radiant energy reaches the bare soil, a relatively large part of this energy is associated with heating and cooling of the upper soil layers. An accurate description of long-term thermal dynamics of such a sparse canopy surface requires a proper description of the heat transfer into the soil. Since large temperature gradients can be present near the surface for strongly illuminated, dry

soils, the description of the soil heat flux depends importantly on the selected number and thickness of the soil layers, and the parametrization of the thermal conductivity of the soil.

The third issue involves evaporation from, and dew to, a sparse-canopy surface. The water-vapour transport from a sparse-canopy surface into the atmosphere is a mixture of transpiration from the canopy elements and evaporation from the bare-soil component or from intercepted water. During the process of dew, water vapour is transported downward from the atmosphere (dew-fall), or condensates immediately after being released by the underlying soil (dew-rise). Treatment of the transfer of water from deeper soil layers into the atmosphere via transpiration plays a significant role in the long-term predictions of cloud development, precipitation, evaporation and soil moisture content (Milly and Dunne 1994).

This paper is dedicated to a comparison of various SVAT schemes using a common data set collected over a sparse vineyard canopy surface for five consecutive days, with particular attention to the issues addressed above. The SVAT schemes include a one-layer model currently in use in the European Centre for Medium-Range Weather Forecasts (ECMWF) global weather-prediction model (Viterbo and Beljaars 1995) and two dual-source models, published by Choudhury and Monteith (1988) and Deardorff (1978). In each of these models the algorithms to describe soil heat-flux density and aerodynamic transfer are based on different physical concepts. A qualitative and quantitative evaluation of these different process treatments is of interest as these algorithms are often applied in large-scale atmospheric models.

Both in nature and in the model simulations the governing parameters show many complex feedbacks, and individual processes cannot easily be investigated in an isolated way. Model errors related to one process of the transfer between surface and atmosphere can cause significant discrepancies for the description of other processes. Despite this feature, the comparison between the models and the observations will be separated into three process categories: soil heat-flux density, aerodynamic exchange of heat, and evaporation and soil-water balance.

2. Description of the SVAT schemes

In this section a brief qualitative description of the SVAT schemes used for the comparison is given. The description addresses the basic characteristics of the models. More details and equations can be found in the original papers. Symbols used in the text and figures are explained in an appendix.

(*a*) *The ECMWF scheme*

The scheme published by Viterbo and Beljaars (1995, hereafter VB95) is currently in use in the ECMWF global weather-forecast model. The model is an improved version of the scheme presented by Blondin (1991). The long-term soil moisture transport was incorrect in the older version, and validations using data collected during FIFE*, in Cabauw and the Amazonian Rainforest Meteorological Experiment showed the current version to be superior in that aspect.

The energy input to the surface-energy balance is provided by the incoming short-wave and long-wave radiation, computed from radiative-transfer calculations for the higher atmospheric layers. Prescribed values of the surface albedo and surface emissivity are used to compute the net radiation as a function of the surface temperature, T_{sur}.

* First ISLSCP (International Satellite Land-Surface Climatology Programme) Field Experiment

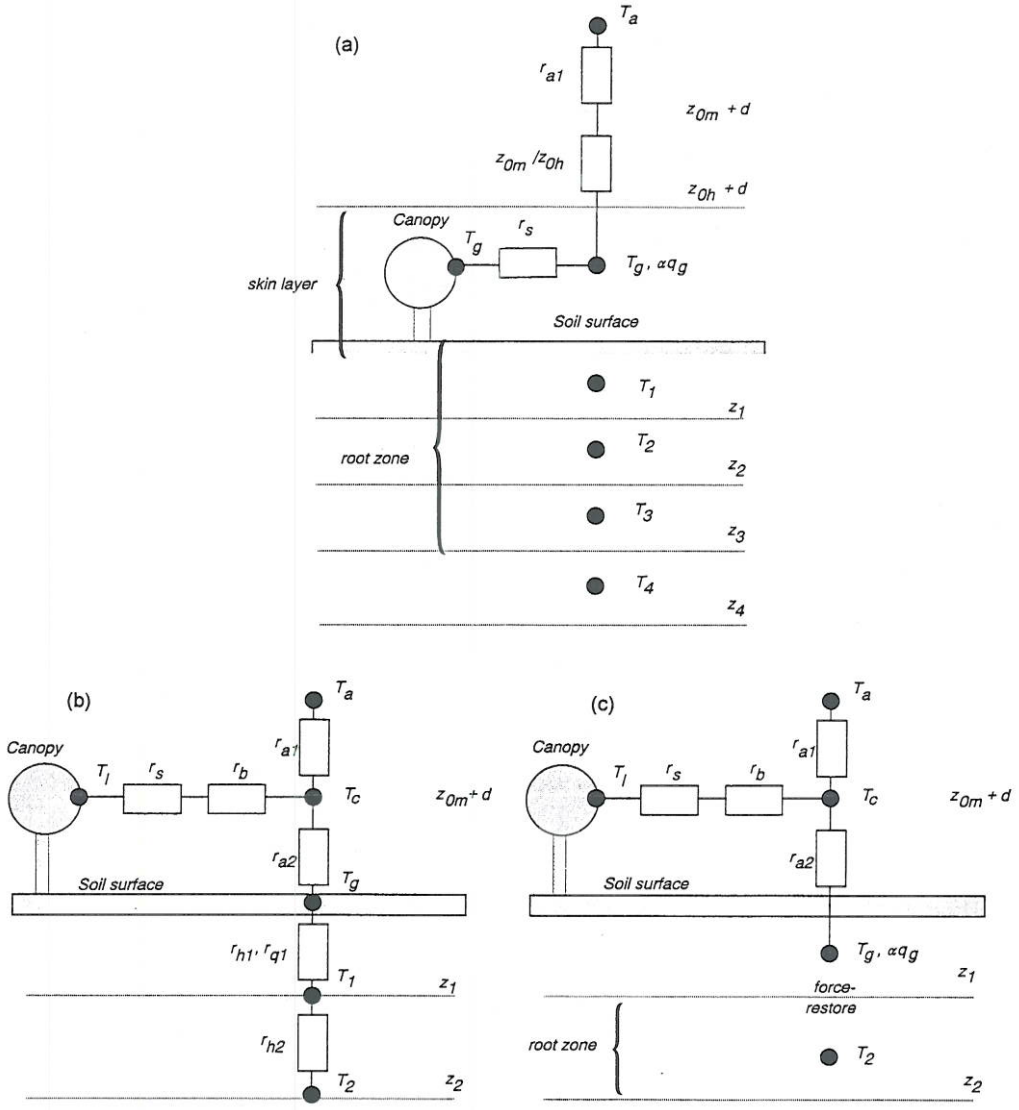

Figure 1. Schematic representation of the models of (a) Viterbo and Beljaars (1995), (b) Choudhury and Monteith (1988) and (c) Deardorff (1978). (See appendix for symbol explanation). Crop resistance r_s and soil resistance r_{ql} apply for water-vapour transfer only, while soil heat resistance r_{h1} is applicable for heat only. All other resistances apply for the transfer of both sensible and latent heat.

The surface scheme consists of four soil layers and a single skin layer without heat capacity (see Fig. 1(a)). The latter has three different sources of latent heat (open water, dry vegetation and bare soil) with a uniform aerodynamic transport to the reference level, but different resistances to account for variable stomatal aperture and low relative humidity of the top soil. The parametrization of the vegetation is very similar to the model proposed by Noilhan and Planton (1989). Soil evaporation is computed using a so-called α-type resistance model (Kondo *et al.* 1990). The soil relative humidity, α, is computed as a function of the soil moisture content in the top soil layer, θ_1.

A different exchange resistance for scalars and momentum between the surface and the reference level is accounted for by taking $z_{0m}/z_{0h} \neq 1$. The temperature of the entire surface layer is unique, and no distinction is made between sensible-heat transfer from either of the three components. The surface temperature is solved iteratively together with net radiation and the energy fluxes at the surface. In VB95 soil heat-flux density is simulated using the temperature difference between the skin layer and the top soil layer, and an apparent conductivity, Λ, of this skin layer. The parameter Λ expresses the heat conductance into the soil through the vegetation layer and the upper soil layer for a given temperature difference between the skin layer and the upper soil layer. A constant value of 7 W $m^{-2}K^{-1}$ is suggested for Λ to give 'reasonable values of the diurnal soil heat flux and surface temperature course'. The four soil layers extend to a depth of almost 3 m, and both heat and moisture transport in the unsaturated zone are simulated using implicit solutions of the relevant partial-differential equations. At the lower boundary a zero-flux condition is assumed for soil heat, and the water flux is equal to the free drainage rate. Hydraulic and thermal diffusivity and conductivity depend on soil moisture content and are parametrized as proposed by Noilhan and Planton (1989).

(*b*) *The scheme of Choudhury and Monteith*

The model of Choudhury and Monteith (1988, hereafter CM88) is based on the two-layer surface model presented by Shuttleworth and Wallace (1985, see Fig. 1(b)). Unlike the Shuttleworth and Wallace scheme, a soil heat-flux density is explicitly parametrized, and an expression is given for the resistance regulating the soil evaporation introduced by Shuttleworth and Wallace (1985).

Two sources of sensible and latent heat are present above the ground: the canopy and the underlying soil. The partition of available radiant energy between sensible- and latent-heat flux is solved using the Penman–Monteith equation for both sources. The available energy, equal to net radiation minus soil heat-flux density, is distributed between the two sources using a radiant extinction as a function of LAI. Unlike VB95, net radiation is prescribed rather than dependent on the surface temperature.

Two soil layers are present, of which the lowest is assumed to be saturated with water. Soil evaporation takes place at the intersection of the two layers, at depth z_1, and the transfer of water vapour through the upper soil layer is regulated by a resistance, proportional to z_1 and the hydraulic diffusivity. Also, the soil heat-flux density is parametrized using the temperature difference between the surface and z_1 and a resistance, which is a function of the soil heat conductivity and the depth of the upper layer. This depth increases at a rate proportional to the soil evaporation rate, in order to simulate the retreat of the saturated zone as soil water is evaporated into the air. The Penman–Monteith combination equation is used to solve simultaneously for the surface temperature, temperature at z_1, and fluxes of soil heat and soil evaporation. The soil layers have no heat capacity, and dynamic heat storage in the upper soil layer is not simulated.

The temperature and humidity deficit of the air in the canopy layer are explicitly solved as functions of the exchange resistances, the temperature and the humidity deficit at the different model levels, and serve as a transfer junction between the substrate, the canopy and the atmosphere above. The parametrization of the aerodynamic resistances r_{a1} and r_{a2} in CM88 is based on the assumption that momentum and scalars are transferred by the same mechanism. An aerodynamic exchange resistance between the canopy air and the substrate, r_{a2}, is parametrized assuming an exponential decay of the eddy diffusivity profile within the canopy layer, and adopting a roughness length for the bare-soil surface. The level of the junction between the canopy and the soil sources is regarded to be the effective level of the momentum sink. This level is derived from numerical higher-order

closure simulations by Shaw and Perreira (1982), and varies with LAI and canopy height. Exchange between this level and the reference level aloft is computed iteratively to include the effect of thermal stratification on the aerodynamic resistance r_{a1}.

A boundary-layer resistance, r_b, appears between the canopy air and the leaf surface. It is a function of the wind-speed profile within the canopy, and an expression for r_b is developed as a function of a wind-speed attenuation coefficient and LAI. No equivalent resistance is present in the pathway between the canopy air and the soil surface. In the limit of a completely bare soil, the absence of an extra resistance for scalars implies that momentum and scalars are exchanged at the same rate, and so $z_{0m} = z_{0h}$.

(*c*) *The model of Deardorff*

The scheme of Deardorff (1978, hereafter D78) is in use in various GCMs, usually in somewhat modified forms (e.g. Dickinson *et al.* 1986; Noilhan and Planton 1989).

As for the CM88 scheme, a dual-source surface is postulated in D78 (see Fig. 1(c)): the canopy and the underlying soil. The boundary-layer resistance for heat and water-vapour exchange (r_b) is treated somewhat more rigorously than in CM88. The aerodynamic exchange within the canopy is parametrized as a weighted average of the exchange from a bare soil and from a dense canopy, using u_* as the characteristic wind speed within the canopy.

As in VB95 the net radiation is computed from the incoming radiant energy and a solution of the surface and canopy temperatures. Separate energy balances are drawn up for the canopy and the substrate, and the incoming radiant energy is distributed over the two components using the fraction of vegetation cover. The canopy temperature T_1 is found iteratively, while the bare-ground temperature T_g is predicted from a rate of change calculated in the previous time step. A weighting procedure is used to obtain the temperature and humidity deficit within the canopy layer, using the explicit values at the soil surface, the canopy surface and the reference level. A non-iterative stability correction (Louis 1979) is used for the aerodynamic resistance above the canopy. Soil evaporation is computed as a function of the relative humidity in the top soil layer, similar to the approach in VB95.

Both the soil heat and soil moisture transport are treated using the force–restore method (Bhumralkar 1975). A forcing of the sensible heat and moisture transport at the surface is modified by a restoring term depending on the temperature and soil moisture deeper in the soil. Both the forcing and restoring term are functions of coefficients which depend on the soil type and moisture content. D78 cites values of these coefficients for only one type of soil, but Noilhan and Planton (1989) determined the coefficients for the 11 soil types of the USDA* classification, based on the parametrization of Clapp and Hornberger (1978).

3. Description of data, model settings and used forcings

(*a*) *Collected data*

Data were collected during the regional scale EFEDA† experiment (Bolle *et al.* 1993) in a dry, semi-arid, sparsely vegetated vineyard near Tomelloso, La Mancha, Spain. Measurements were taken between 2 and 29 June 1991. The site consisted of a flat extensive vineyard area with a homogeneous fetch exceeding 1.5 km in (prevailing) eastern

* United States Department of Agriculture.

† ECHIVAL (European project on Climate and Hydrological Interactions between the Vegetation, the Atmosphere and the Land surface) Field Experiment in a Desertification threatened Area.

and western directions. The vegetation was formed by a regular grid of individual vine plants (*Vitis Vinifera L.*, cv. Airen), growing rapidly as the measurement season proceeded. During the period of comparison the plants were approximately 1 m high, covered about 10% of the surface and had a LAI of 0.3 m^2m^{-2}. The roots extracted water from a rather compact porous layer extending from a depth exceeding 0.5 m. The deepest point of water extraction by the plants is not known exactly, but root investigations carried out in 1994 suggested that roots were present at depths exceeding 3 m. The soil layer near the surface was a sandy loam soil covered with stones with a typical diameter of 0.03 m. The upper soil layer was very dry and warm during daytime. Virtually no understorey vegetation was present, presumably due to the lack of water in the top soil layer, and regular tillage.

Measurements consisted of both forcings and flux densities to validate model results. Atmospheric forcings were measured at a reference level of 2.95 m height, and consisted of air temperature, air humidity (psychrometer manufactured at the Wageningen Department of Meteorology, WAUMET), horizontal wind speed (WAUMET), incoming and reflected short-wave radiation (Kipp CM5) and net radiation (two Middleton net radiometers, one mounted above a plot of bare soil and one above an individual plant at 1.5 m height). Average net radiation was obtained by simply averaging the readings of the two net radiometers. Long-wave downward radiation $L\downarrow$ was parametrized by closing the surface-radiation balance:

$$Q^* = (1 - a)K\downarrow + L\downarrow - \varepsilon\sigma T_s^4. \tag{4}$$

In Eq. (4), σ is the Stefan–Bolzman constant, the values of global radiation, $K\downarrow$, and net radiation, Q_*, were measured, the albedo, a, and long-wave emissivity, ε, were taken as in the simulations (see below), and an effective surface temperature, T_{sur}, was defined as a weighted average of the measured bare-soil and canopy temperatures (Eq. (2)). Soil temperatures were measured using PT100 resistance thermometers at five levels at depths between 0.03 and 0.50 m. The surface temperature was measured using an infrared sensor mounted at 3 m above the soil surface on a cable and moved along a transect of 35 m. The transect included both canopy elements and bare soil. Individual canopy and bare-soil temperatures were extracted from the record of temperatures.

Aerodynamic roughness, z_{0m}, and zero-plane displacement, d, were determined from wind-profile measurements at four levels between 1.5 and 10.0 m. These quantities changed considerably throughout the measurement period owing to the vegetation growth.

Friction velocity and flux densities of sensible- (H) and latent- (λE) heat were measured using a 3-dimensional Kaijo Denki DAT310 sonic anemometer provided with a copper-constantan thermocouple and a Lyman-α fast response hygrometer, both manufactured at WAUMET. Soil heat-flux density, G, was measured using four TPD soil heat flux plates buried at 5 cm depth, of which two were placed under an individual plant and two under a sunlit soil plot. A weighted average based on the fraction of vegetation cover was used to obtain an average value of G.

All these data were collected on magnetic tape using a datalogger controlled by a PDP11 minicomputer. Data were averaged over 10-minute intervals, and variance and covariance statistics were computed after removing any linear trend over this interval. These 10-minute averages were finally averaged to half-hour values. Soil heat-flux corrections were carried out to account for heat storage above the soil heat-flux plates, and different conductivity between the plates and the surrounding soil. The eddy correlation corrections dealt with wind-vector rotation (McMillen 1988), limited frequency response of the eddy-correlation system (Moore 1986), and contribution of air-density fluctuations to sensible- and latent-heat flux (Webb *et al.* 1980).

Soil moisture measurements were carried out at a few days before and during the comparison period by the Department of Water Resources of the Wageningen University, using Time Domain Reflectometry at 0.10 m intervals to 0.50 m depth (Droogers *et al.* 1993). Leaf resistance to water-vapour transport was measured from sunrise until sunset once every two days using a DeltaT semi-automatic dynamic porometer (AP1). After extensive quality control on data and calibration (Jacobs 1994), a crop resistance was obtained by averaging the measurements using a weighting based on leaf age and light exposure. LAI and f_c were measured by counting the leaves of ten plants every 5 days, and relating these to the average leaf size determined in the field.

(*b*) *Forcings and specific model settings*

The simulations were carried out using observations taken between 2000 GMT 19 June (Day of year (DOY) 170) and 2400 GMT 24 June (DOY 175). For each model the simulation time step was 600 s, and observations averaged to half-hour intervals were interpolated to match the time discretization.

All three models use measured values of temperature, wind speed and humidity at a reference height above the canopy, and initial soil temperature and soil moisture profiles. Observations of total net radiation were used as input for CM88, and short-wave and long-wave incoming radiation for VB95 and D78. However, during the nocturnal periods following DOY 173 and 174 data are missing owing to failure of the measurement system. Linear interpolation was used to estimate missing data. Initial soil moisture and temperature profiles can be found in Table 1 for each of the models. Temperatures and moisture contents in soil layers deeper than measured were assumed to be identical to the values at 0.50 m depth at the starting time of the simulation. Figure 2 displays the atmospheric forcings.

To make the comparison of the models as straightforward as possible, most model settings were adjusted to give similar surface and vegetation specifications for all models. However, since all models treat several parameters differently, some choices had to be made. A summary of all model settings can be found in Table 2.

TABLE 1. INITIAL VALUES OF SOIL TEMPERATURE AND SOIL MOISTURE CONTENT AT VARIOUS DEPTHS FOR EACH MODEL

Parameter	Depth (m)	Model		
		D78	CM88	VB95
Soil temperature (K)	0	293.09	293.09	293.09
	0.07			302.96
	0.10		303.21	
	0.28			298.66
	0.50	296.09	296.09	
	1.00			296.09
	2.89			296.09
Soil moisture content (m^3m^{-3})	0.07			0.07
	0.10	0.07		
	0.28			0.08
	0.50	0.15		
	1.00			0.15
	2.89			0.15

Viterbo and Beljaars (1995). In the original paper of VB95 universal functions describing the physical properties of the soil are used for each soil type. However, we adjusted these parameters according to the suggestions made by Noilhan and Planton (1989) for a sandy

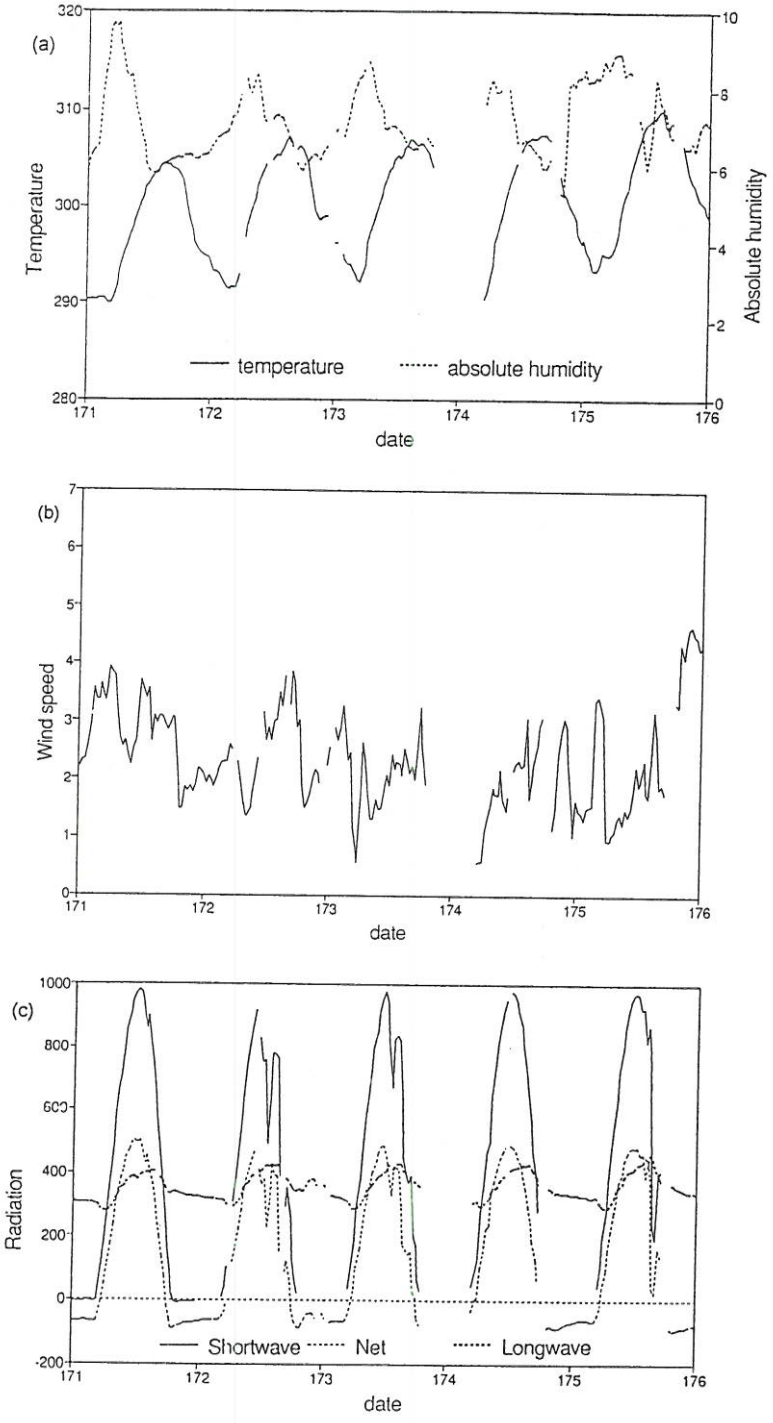

Figure 2. Meteorological forcings: (a) temperature (K) and humidity (g m^{-3}), (b) wind speed (m s^{-1}), and (c) short-wave, long-wave and net radiation (W m^{-2}) for days 171–176 of 1991.

TABLE 2. SUMMARY OF MODEL SETTINGS

		Model		
Parameter	Symbol	D78	CM88	VB95
Time step (s)	t	600	600	600
Crop height (m)	h	1	1	—
Roughness length (m)	z_{0m}	Functions of LAI, h, C_D	Functions of LAI, h, C_D	0.035–0.043
Displacement height (m)	d	Functions of LAI, h, C_D	Functions of LAI, h, C_D	0.35
Soil roughness length (m)	z_0'	0.01	0.01	—
Roughness length for heat (m)	z_{0h}	—	—	$z_{0m}/200$
Leaf drag coefficient	C_D	0.2	0.2	—
Reference height (m)	z_R	2.95	2.95	2.95
Soil albedo	a	0.29	—	0.29
Canopy albedo	a	0.29	—	0.29
Surface emissivity	ε	0.98	—	0.98
Depth of soil layers (m)	z_1	0.10	0.40 (start)	0.07
	z_2	0.50	0.50	0.28
	z_3	—	—	1.00
	z_4	—	—	2.89
Skin conductivity ($W\,m^{-2}K^{-1}$)	Λ	—	—	7
Characteristic leaf size (m)	l	0.05	0.05	—
Extinction coefficient for net radiation	α_{Q^*}	—	0.7	—
Extinction coefficient for wind speed	α_u	—	3	—
Extinction coefficient for eddy diffusivity	α_K	2.5	2.5	—
Min crop resistance ($s\,m^{-1}$)	$r_{c,min}$	125	—	240
Cuticular conductance ($m\,s^{-1}$)	g_0	—	0.0005	—
Change of conductance per unit shortwave radiation ($m\,s^{-1}$ per $W\,m^{-2}$)	g_1	—	4×10^{-6}	—
Thermal conductivity top soil layer ($W\,m^{-1}K^{-1}$)	λ_1	Functions of θ_1	0.3	Functions of θ_1
Thermal conductivity other soil layers, i ($W\,m^{-1}K^{-1}$)	λ_2	Functions of θ_2	0.5	Functions of θ_1
Retention curve coefficient	b	4.90	—	4.90
Saturated soil moisture ($m^3\,m^{-3}$)	θ_{sat}	0.472	0.472	0.472
Field capacity (m^3m^{-3})	θ_{cap}	0.354	—	0.354
Wilting point (m^3m^{-3})	θ_{wil}	0.075	—	0.075
Tortuosity	τ	—	2	—
Saturated hydraulic pressure (m)	Ψ_{sat}	−0.25	—	−0.25
Saturated hydraulic conductivity ($m\,s^{-1}$)	$\lambda_{h,sat}$	3.41×10^{-5}	—	3.41×10^{-5}
Leaf-area index	LAI	0.29–0.35	0.29–0.35	0.29–0.35
Fraction vegetation cover	f_c	0.10–0.12	0.10–0.12	0.10–0.12

loam soil type (see Table 2). The surface albedo was fixed at the measured value 0.29 for both the vegetation and soil component, and for the long-wave emissivity a value of 0.98 was taken (Bolle and Streckenbach 1993). In the operational ECMWF version of VB95, roughness lengths for heat and momentum are specified quantities for each grid box. Here, calculated aerodynamic roughness and zero-plane displacement were taken.

The value of z_{0m} increased from 0.035 m at DOY 171 to 0.043 m at DOY 175, whereas d was kept constant at 0.35 m in this limited time range. Following Verhoef *et al.* (1994, personal communication), a different aerodynamic roughness for heat was calculated, using $z_{0m}/z_{0h} = 200$. Note that this value is an order of magnitude larger than the value suggested by Braud *et al.* (1993), who simulated the energy balance of a similar sparsely vegetated vineyard using the scheme of Noilhan and Planton (1989). Since the sensible-heat flux is the dominant term of the surface-energy budget for a dry sparse-canopy surface, the choice for z_{0m}/z_{0h} will reflect the difference between the mean level of the momentum sink (the canopy elements) and the heat source (the underlying bare soil). The apparent conductivity of the skin layer was kept at the suggested value of 7 W $m^{-2}K^{-1}$. Since exact information about the root distribution was not available, the rooting depth of the vegetation was defined according to the original suggestion (1 m, with water extracted equally from the top three layers). The response of the canopy resistance to light and soil moisture was parametrized according to VB95. No stomatal dependence on air temperature or air humidity is taken into account in VB95. LAI was transformed in the leaf area per area covered by plants by dividing the measured LAI by the measured f_c. In the simulation period, LAI increased from 0.29 m^2m^{-2} on DOY 171 to 0.35 m^2m^{-2} on DOY 175, whereas f_c increased from 0.10 to 0.12 in the same period.

Choudhury and Monteith (1988). CM88 uses principally net radiation, wind speed, humidity and air temperature as forcing functions. For this comparison, the deep-soil temperature was taken from measurements at 0.50 m depth, rather than taking it as constant. The initial depth of the top soil layer was taken to be 0.40 m, to get a high soil-evaporation resistance corresponding to a small soil evaporation expected from a dry soil surface. The absence of a saturated zone near the surface made a formal justification for this choice impossible. For the thermal conductivity in the top layer a value of 0.3 W $m^{-1}K^{-1}$ was adopted, and in the bottom layer 0.5 W $m^{-1}K^{-1}$, following Verhoef *et al.* (1995). Directly measured values of LAI and crop height, h, were adopted. Roughness length and displacement were computed as functions of LAI and h, assuming a leaf drag coefficient of 0.2 (CM88). Characteristic leaf size, necessary for computing r_b, was 0.05 m, and h was kept constant at 1 m. Since explicit calibration coefficients of the response function for stomata to radiation are not given by CM88, the function was calibrated using porometry measurements taken at several days in the measurement period (see Table 2).

Deardorff (1978). For D78, z_{0m} and d were computed using the same formulation as CM88. The thickness of the top soil layer was fixed at 0.1 m, and the deep-soil temperature varied with a seasonal cycle as suggested in the original paper. The crop resistance was parametrized as a function of radiation, air temperature, atmospheric humidity and soil moisture, following the general suggestions made by Noilhan and Planton (1989).

Similar soil physical quantities were taken as for VB95, that is, the sandy loam soil type (see Table 2). The parametrization of the surface albedo as a function of soil moisture content was replaced by the observed value (0.29), and the surface long-wave emissivity was taken to be the same as in VB95 (0.98 for both plants and soil).

4. Simulations with the SVAT schemes

The sparse-canopy surface for which the simulation was carried out has some pronounced properties with respect to the partition of energy over the various components. First, unlike in the case of densely vegetated surfaces, the soil heat-flux density is an important component of the surface energy balance for the current data set. Owing to the small relative area covered by the plants (maximum 12%), approximately 30% of the total

daytime net radiation was used to heat the soil. The daily averaged soil heat-flux density was approximately 20 W m^{-2}, indicating a temperature increase in deeper soil layers at this time of the year.

Second, the surface net radiation is hardly used for evaporation (< 10% of net radiation, generally), but a clear distinction between the canopy and the underlying soil is present in terms of latent- and sensible-heat exchange and surface temperature. Sensible heat (about 60% of net radiation) was released mainly by the warm substrate, whereas the evaporation, which was dominated by the canopy, caused the vegetation to be significantly cooler than the surrounding bare soil.

Third, the large rooting depth enabled the vegetation to transpire in spite of a very dry top soil. Stomatal responses to the moisture content in the top soil layer are expected to be small.

The models faced the challenge of simulating these features. The simulations will be compared with attention focused on three aspects: soil heat-flux density, sensible-heat transfer between the surface and the atmosphere, and evaporation in combination with soil moisture budget.

(*a*) *Soil heat-flux density*

Figure 3 gives the measured and simulated soil heat-flux density for DOY 171–175. As can be seen, the differences between the model predictions are very large. D78, using a force-restore method to compute the soil heat-flux density, gives a very good agreement with observations. A small underestimation is present early in the comparison period. The relatively slow response of the soil temperature to surface forcings results in a clear phase shift of the soil heat-flux density compared with net radiation (detailed in Fig. 4), which is well simulated by D78.

Also VB95 simulates a maximum soil heat-flux density somewhat before local noon, albeit less pronounced than D78. The soil heat-flux density is on average about 30% too small compared with the observations. This underestimation is not caused by a discrepancy between the observed substrate temperature and the simulated skin-layer temperature (Fig. 5). Obviously, the chosen value of the skin conductivity, Λ, plays a significant role in this aspect.

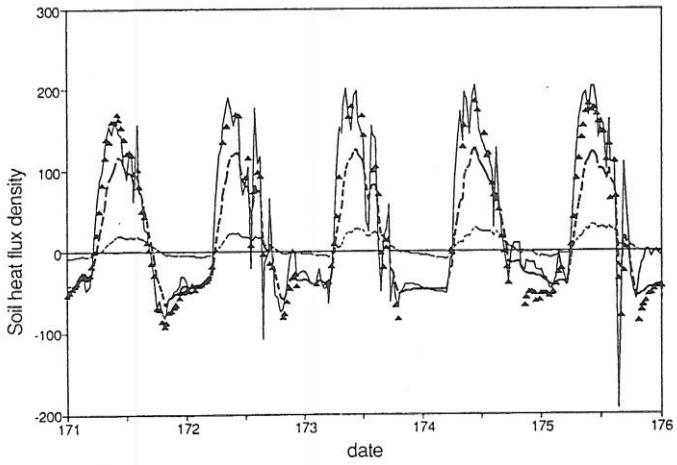

Figure 3. Soil heat-flux density (W m^{-2}) for all comparison days (i.e. days 171–176 of 1991): ▲ observations; and the models of —— Deardorff (1978); – – – Viterbo and Beljaars (1995); and - - - - Choudhury and Monteith (1988).

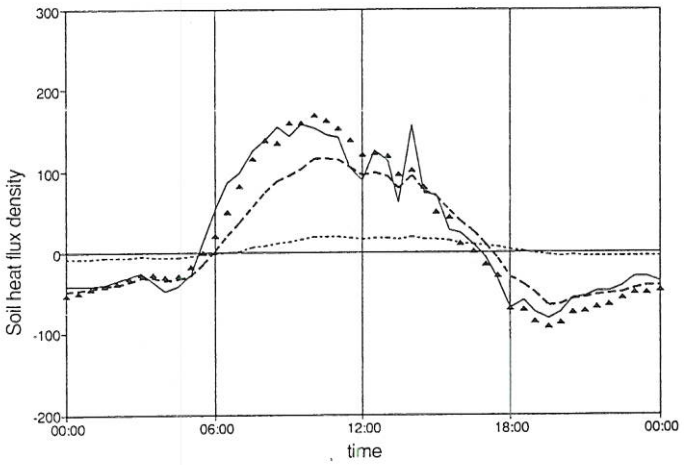

Figure 4. Measured and simulated soil heat-flux density (W m^{-2}) for day 171 of 1991; symbols as in Fig. 3.

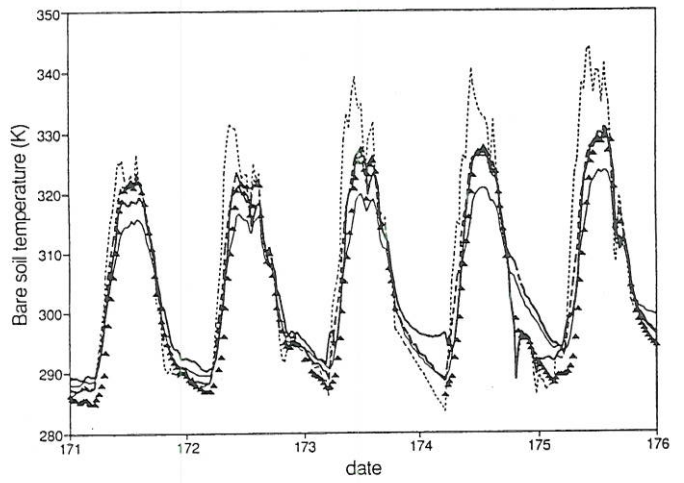

Figure 5. Measured and simulated bare-soil temperature for days 171–176 of 1991 for the models of Choudhury and Monteith (1988) (CM88) and Deardorff (1978) (D78), and skin temperature for Viterbo and Beljaars (1995) (VB95); ▲ observations; —— (D78); – – – (VB95); - - - - (CM88); and —— (CM88) with soil heat-flux density from D78 (see text).

The soil heat-flux density predicted by CM88 is much too small compared with the observations, in spite of using measured values of the thermal conductivity in the two soil layers (see Table 2). The underestimation is almost a factor 10, and is too large to be related to the choice of the initial dry soil-layer depth (z_1). Taking $z_1 = 0.01$ m rather than 0.40 m at the first time step increases the soil heat flux by only a few per cent (figures not shown). Also, a phase shift with respect to the local noon is not simulated by CM88 (see Fig. 4). Only by increasing the thermal conductivity to unlikely high values (exceeding 5 W $m^{-1}K^{-1}$ for the top soil layer) can the maximum of the simulated soil heat flux be matched to the maximum of the observed values, but not at the right time with respect to the local noon. The reason for the discrepancy between model and data is the absence of a heat capacity in the upper soil layer. The use of a resistance to regulate the heat flux in

CM88 implies that no heat loss occurs in this layer. Hence, the soil heat flux will always respond immediately to the forcing at the surface, and a phase shift will not be present in the calculations.

As a result of the underestimation of the predicted soil heat-flux density by CM88 (Fig. 3), a large part of the net radiation is available for λE and H, and causes a clear overestimation of these two terms. This overestimation is reflected in the plot of the simulated substrate temperature, shown in Fig. 5, which is high compared with the radiometric observations of the bare-soil temperature. The overestimation of the prediction of H and λE makes a comparison of the parametrization of, for example, the aerodynamic exchange by CM88 with other models impossible. With respect to this aerodynamic exchange a fair comparison between CM88 and D78 is particularly useful, since these models use different formulations for aerodynamic resistances in a similar resistance network (Figs. 1(b) and 1(c)). Therefore, in the following, the computed soil heat-flux computation in CM88 is replaced by values of G as computed by D78, which are very close to the observations (Fig. 3). A comparison of H and λE from CM88 and VB95 is somewhat biased by the difference of G computed by D78 and VB95, and must be carried out with caution. The soil evaporation in CM88 is treated as before, using a resistance for water-vapour transfer at the soil surface interface which increases as soil evaporation progresses. A model of this form is essentially comparable with the model presented by Shuttleworth and Gurney (1990), who adapted the original two-layer model of Shuttleworth and Wallace (1985) with the parametrization of the aerodynamic parameters according to CM88.

(*b*) *Sensible-heat exchange and surface temperature*

For the surface considered the aerodynamic exchange of heat between the surface and the reference level is dominated by the contribution of the bare-soil component. This exchange can be separated into two segments for each model: a transfer above the canopy equivalent to momentum transfer, and an extra resistance to account for the difference between heat and momentum transport. In VB95 this difference is accounted for by taking $z_{0m}/z_{0h} > 1$, while in CM88 and D78 this extra resistance consists of r_b and r_{a2} (see Fig. 1).

The aerodynamic resistance above the canopy, r_{a1}, is a function of the reference wind speed, the roughness length z_{0m} and a stability correction. The estimation of z_{0m} from LAI and h as applied in CM88 and D78 resulted in a value of 0.082 cm at DOY 171, slowly increasing to 0.095 cm at DOY 175, overestimating the observed roughness length by a factor 2. The measured friction velocity, u_*, was overestimated by CM88 and D78, and reproduced very well by VB95 (figure not shown). The latter was to be expected from the adoption of measured values of z_{0m}. The slightly different stability corrections in CM88 and D78 hardly resulted in different values of u_* and r_{a1}.

Figure 6 shows the values of the aerodynamic resistance between the soil and the canopy layer (r_{a2}, for D78 and CM88) and the excess resistance applicable for $z_{0m}/z_{0h} = 200$ for VB95, for unstable conditions. A clear difference between CM88 and D78 is present in the values adopted for r_{a2}, CM88 giving a value roughly twice as high as D78. The CM88 parametrization corresponds closely to the excess resistance adopted by VB95 for daytime situations. The implications of the parametrization of r_{a2} and the excess resistance are demonstrated well by the relationship between the bare-soil temperature and the total sensible-heat-flux density, since the sensible heat released by the canopy is only a small part of the total sensible-heat exchange. CM88 and VB95 succeed very well in predicting both the total sensible-heat-flux density (Fig. 7) and the bare-soil temperature (Fig. 5). D78 underestimates the bare-soil temperature by at most 7 degC around noon, and overestimates

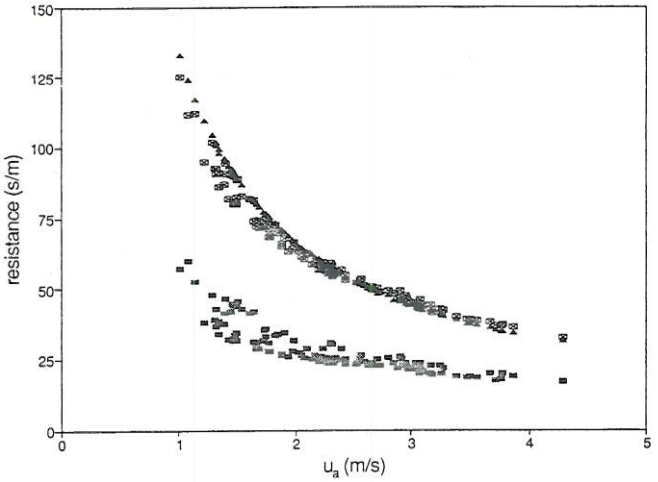

Figure 6. Aerodynamic resistance within the canopy for the models of Deardorff (1978) (■) and Choudhury and Monteith (1988) (▲), and excess resistance for Viterbo and Beljaars (1995) (⊠), as a function of measured wind speed at the reference level, u_a. Only simulation points are shown for sensible-heat-flux density $H > 0$.

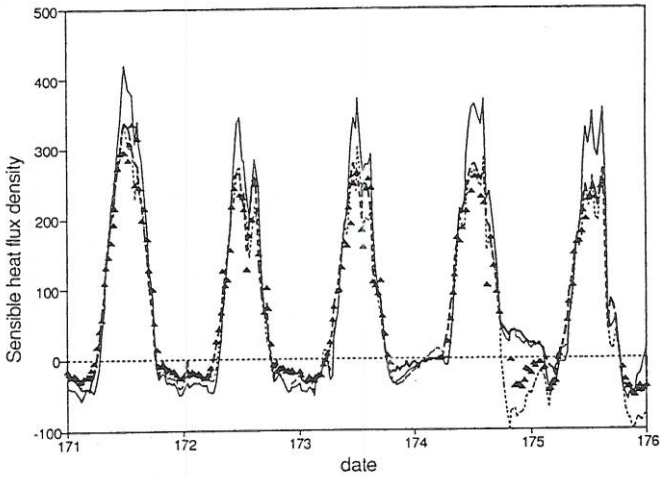

Figure 7. Measured and simulated total sensible-heat-flux density (W m^{-2}); symbols and data as in Fig. 3.

the sensible-heat-flux density by up to 100 W m^{-2}. A small part of this overestimation is associated with an enhanced net radiation due to lower surface temperatures.

The performance of VB95 is very good for both sensible-heat flux and surface temperature, since values of z_{0m} and z_{0h} were obtained from field measurements. A small overestimation of the sensible-heat-flux density is present for the first simulation day. Obviously, the choice for the value of z_{0m}/z_{0h} is an important parameter for a proper description of the sensible-heat transfer between the surface and the atmosphere. An evaluation of z_{0m}/z_{0h} using the model of CM88 as outlined in Eqs. (1)–(3) reveals a clear variation as time proceeds, both diurnally and for the five consecutive days (Fig. 8). A clear increase during the day can be seen, which can be interpreted as a reduction of the effective level of the sensible-heat source as the bare ground gets warmer. Taking $z_{0m}/z_{0h} = 200$ for the whole period appears a good estimate for all days except the first.

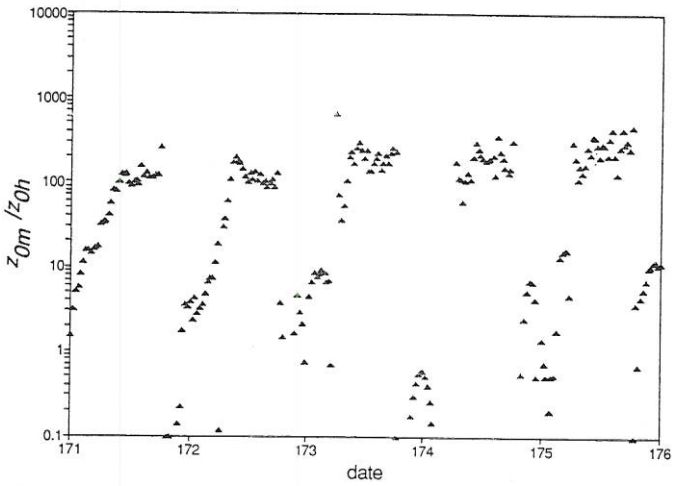

Figure 8. Computed ratio of z_{0m}/z_{0h} using the model of Choudhury and Monteith (1988) with observed values of G, and a linear interpolation for obtaining the effective surface temperature T_{sur} (see text and appendix for explanation of symbols) for days 171–176 of 1991.

(*c*) *Evaporation and soil water budget*

VB95 and D78 underestimate the total evaporation during the entire comparison period, while CM88 gives a small but consistent overestimation (Fig. 9(a)). The evaporated water originates almost entirely from the canopy in CM88, since soil evaporation is limited to low values by selecting a large top-soil-layer depth (Fig. 9(b)). Unlike CM88 and VB95, D78 starts to compute a significant soil evaporation on later days, especially in the early hours after sunrise. The strong diurnal variation of the moisture content in the top soil layer, θ_1 (Fig. 10) causes the humidity at the soil surface to reach values which are higher than the humidity in the canopy layer, giving rise to pronounced soil evaporation. Once the top soil layer has lost some water to the air, the relative humidity at the soil surface drops quickly, and soil evaporation suddenly ends.

Owing to the different vertical resolution of the numerical schemes used to describe the soil moisture content adopted by VB95 and D78, the dynamics of the top-soil moisture content, θ_1, differ significantly for both models. In D78 θ_1 is much lower than the moisture content in the soil layer below, while this difference is small in VB95 (Fig. 10). As a result, diurnal variations of θ_1 are strongly damped in VB95. The calculated soil moisture content in the root zone decreases much stronger in VB95 (layers 1–3) than in D78 (both model layers), in spite of a similar canopy evaporation rate (see below). The stronger decrease in VB95 is a direct result of the simulation of water drainage to lower soil layers, not accounted for in D78. For longer-term predictions these different approaches can lead to significant differences in predicted soil moisture content in the root zone. Unfortunately, the measurements of θ are taken only once during the comparison period, and these values were used to initialize the model runs. Therefore, a detailed comparison between model runs and observations is not possible.

The canopy evaporation rate is predicted rather differently by the various models. Since the crop resistance is usually approximately an order of magnitude larger than the other resistances in the pathway between the canopy and the reference level, the parametrization of r_s is of critical importance for the prediction of the canopy evaporation. Figure 11 shows values of computed crop resistances, combined with data from weighted averaged porometry measurements. Also shown are values of r_s obtained from

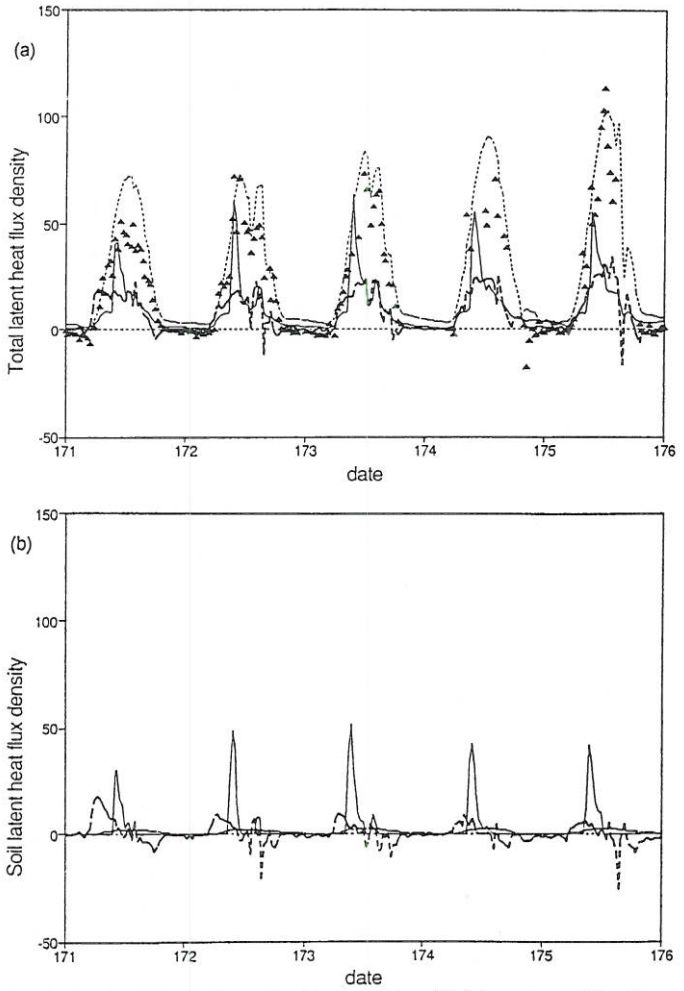

Figure 9. Measured and simulated latent-heat-flux density (W m^{-2}) (a) total and (b) soil; symbols and time as in Fig. 3.

measured evaporation rates and leaf temperatures, by assuming zero soil evaporation and adopting parametrizations for r_b and r_{a1} according to CM88. The values of r_s predicted by CM88, which are a function of incoming radiation only and calibrated using measurements, obviously agree best with both directly measured and inferred values. The formulations for soil moisture stress and response to air humidity adopted by VB95 and D78 result in higher values for r_s. Note that in spite of the higher crop resistance in VB95 compared with D78, the canopy evaporation rate of the two models is similar. In VB95 the surface humidity is considerably higher than the humidity at the canopy surface in D78 during daytime, owing to the uniform high skin-layer temperature.

Another reason for the difference in canopy evaporation between D78 and CM88 is the difference in parametrization of net radiation absorbed by the vegetation (Fig. 12). The exponential extinction formulation adopted by CM88 gives higher values for the energy available to the canopy than the explicit solution of the separate soil and canopy energy balances as modelled by D78. Hence, a higher canopy-evaporation rate will be predicted by CM88 when all other variables remain unchanged.

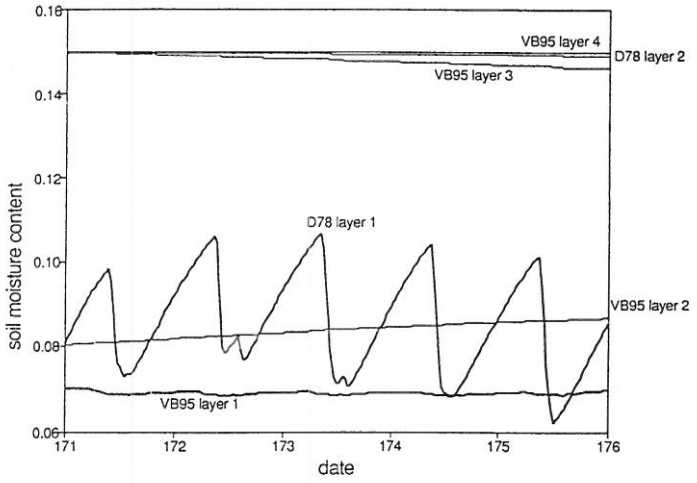

Figure 10. Soil moisture content (m^3m^{-3}) as simulated by the models of Deardorff (1978) (D78) and Viterbo and Beljaars (1995) (VB95) for days 171–176 of 1991. Labels refer to model layer numbers, and the top layers are indicated by heavy lines.

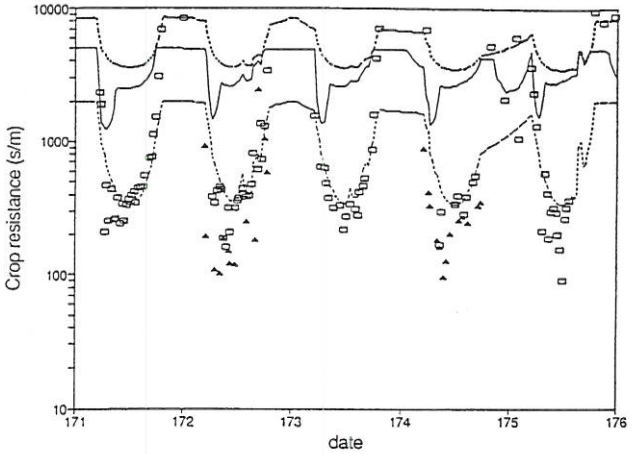

Figure 11. Measured and simulated crop resistance. Observations are carried out with a dynamic diffusion porometer (▲) and inferred from measured latent-heat-flux density and assuming no soil evaporation (□). Indicated lines of simulations and time as in Fig. 3.

5. Discussion and conclusions

A comparison of three schemes for describing the exchange of momentum, heat and water vapour at the atmosphere–surface interface for a sparse-canopy surface shows a wide range of predicted results. In particular, predicted values of soil heat-flux density and surface evaporation vary widely.

With respect to the soil heat-flux density, the parametrization of D78 gives the best results compared with data. The simple resistance approach of CM88 underestimates the soil heat-flux density by almost an order of magnitude, owing to neglecting dynamic heat storage in the upper soil layer. A dynamic heat storage, ΔG, can be implemented in the model of CM88, by taking the heat necessary to change the temperature of the upper soil layer into account while solving the temperatures at the surface and at the interface between

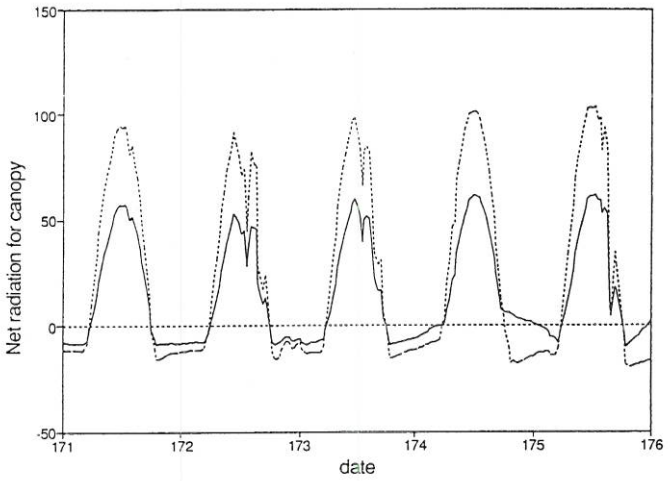

Figure 12. Amount of net radiation (W m^{-2}) absorbed by the canopy layer parametrized by the models of Deardorff (1978) and Choudhury and Monteith (1988). Indicated lines of simulations and time as in Fig. 3.

the two soil layers, at depth z_1. A simple description of this extra energy storage in the top soil layer could be postulated by assuming that the temperature of the top soil layer changes uniformly with depth during the simulation time step. This approach is similar to the computation of the heat storage in a well-mixed water reservoir (see Keijman 1974). However, the effect of ΔG on the total soil heat-flux density strongly depends on the choice for z_1, since the well-mixed criterion is used. In a real soil this criterion is never met, and a good estimate of G will only be achieved by a smart choice of z_1, without the possibility for providing a universal solution.

VB95 also underestimates soil heat-flux density, by approximately 30%. Much of this underestimation is due to the choice of the value for the apparent heat conductivity of the skin layer, Λ. This parameter is defined as the flow of heat per degree temperature difference between the upper soil layer and the skin temperature. For a dense canopy, the presence of the vegetation will thermally isolate the soil from the atmosphere, and Λ may be expected to be small. For a sparse canopy, however, this temperature difference can be regarded as proportional to the soil-temperature gradient immediately below the surface. Then, Λ is related to a physical thermal conductivity, λ (dependent on soil type), according to

$$\Lambda \Delta T = (\Lambda \Delta z)\frac{\Delta T}{\Delta z} \approx \lambda \frac{\partial T}{\partial z} \tag{5}$$

where Δz is a reference depth. Obviously, a value of Λ could be chosen corresponding to the soil type under investigation which would give a better prediction of G. A first guess for the value of Δz would be the level where T_1, the temperature of the top soil layer, applies. For a linear soil-temperature profile this would be the centre of the top soil layer (0.035 m), but for steep gradients with an exponential shape this level is expected to be closer to the surface at, say, 0.015 m. For a given thermal conductivity of approximately 0.3 W $m^{-1}K^{-1}$, a value of 20 rather than 7 W $m^{-2}K^{-1}$ would be a more appropriate estimate for Λ in the current situation.

In all tested models the surface temperature plays a key role, since it regulates important processes such as soil heat flux, sensible- and latent-heat flux, and in a minor sense net radiation. CM88 predicts high sensible-heat fluxes in the original form, since surface temperatures are strongly overestimated when too little heat is transported into

the soil. However, when the soil heat-flux density was forced to values simulated by D78, their parametrization of the aerodynamic exchange within the canopy (using the resistance labelled r_{a2}) appeared to give better results of the surface temperature than the formulation used by D78. In CM88, the total exchange resistance for heat between the bare soil and the reference level resembles the value included in VB95, which was based on field measurements of roughness length, surface temperature and sensible-heat flux. D78 prescribes a value of r_{a2} which is about half as high as CM88, and consequently underestimates the bare-soil temperature.

The parametrization of aerodynamic transfer of heat is especially important for a sparse canopy like the vineyard under investigation, where during daytime high sensible-heat fluxes from the bare-ground component occurred. The heat transfer is dominated by the soil component, but it is governed by many meteorological parameters in the partitioning of available energy between the soil and the vegetation. From the current exercise it can be seen that when the aerodynamic transfer between the atmosphere and a sparsely vegetated surface is treated as an excess resistance for heat, its value cannot be expected to be constant, as was discussed by Kustas *et al.* (1989), and Blyth and Dolman (1995). However, for the limited simulation period investigated in this study, a constant value of $z_{0m}/z_{0h} = 200$ as applied in VB95 yields satisfactory results with respect to both surface temperature and sensible-heat-flux density.

The crop resistance for evaporation is best described by CM88, where a calibrated function of incoming radiation was used to describe r_s. The dependence of r_s on soil moisture content cannot be expected to be realistically described by either D78 or VB95, which assume a much smaller root zone than found in the field. Also the response of stomatal aperture to ambient humidity deficit is not fully resolved, and is an issue of discussion. Under dry and warm conditions, several plant species seem to develop a specific survival mechanism, and respond differently to air humidity than plants from which the expression of Noilhan and Planton (1989) was obtained (Monteith 1995).

The partition of radiant energy over the vegetation and the underlying substrate is solved in two different ways by CM88 (adopting radiant extinction) and D78 (solving separate energy balances for the two surface components). The extinction parametrization was originally developed for closed canopies, and is expected to deviate significantly from real radiative interception for a vegetation stand with widely separated plants. On the other hand, drawing up separate radiation balances does not take all edge effects into account. Which of the parametrizations is to be preferred can only be supported by detailed measurements and modelling efforts, and will most likely be different for each type of vegetation.

For large-scale application a land-surface scheme necessarily needs to describe a wide range of land-surface types, covering the full transition from densely vegetated to completely bare, accurately. From the current study, a general conclusion can be made that for a rather sparsely vegetated surface none of the three models compared can be regarded to be the 'ideal' land-surface scheme. Each of the schemes involved in this test has some superior qualities compared with the others, but also shows significant deficiencies when applied to a very sparse canopy. For the surface for which this comparison was run, a combination of parts from each of the models will likely give optimal results. Following the conclusions above such a combined model would consist of a soil-heat-flux parametrization using the force–restore method, an aerodynamic exchange process simulated using the resistance formulation of CM88, and a canopy resistance parametrization that realistically accounts for stomatal responses to soil moisture content and air humidity. The development and test of such a model will be discussed in a future paper.

Acknowledgements

The authors are indebted to the technical staff at the Wageningen Meteorology Department for their help in collecting and processing the data. Anton Beljaars is acknowledged for his constructive discussions. Two anonymous referees spent considerable time and effort to improve the manuscript, and this is greatly appreciated. The first and second author were supported by grants from the Dutch NWO under contract numbers 752-365-030 and 752-365-037, and by the European Economic Community under contract number EPOC-CT90-0030.

Appendix

List of symbols used

Main symbols:

d	zero-plane-displacement height (m)
f	relative fraction (−)
G	soil heat-flux density (W m^{-2})
H	sensible-heat-flux density (W m^{-2})
h	crop height (m)
$K\downarrow$	incoming global radiation (W m^{-2})
L	Monin–Obukhov length (m)
$L\downarrow$	incoming long-wave radiation (W m^{-2})
LAI	leaf-area index (−)
Q_*	net radiation (W m^{-2})
q	specific humidity (kg kg^{-1})
r	resistance (s m^{-1})
T	temperature (K)
u	wind speed (m s^{-1})
u_*	friction velocity (m s^{-1})
z	level (m)
α	relative humidity of surface soil moisture content (−)
ε	long-wave emissivity (−)
θ	soil moisture content ($m^3 m^{-3}$)
κ	Kármán constant
λ	soil thermal conductivity (W $m^{-1} K^{-1}$)
λE	latent-heat-flux density (W m^{-2})
Ψ	stability function (−)
σ	Stefan–Bolzmann constant (W $m^{-2} T^{-4}$)
ρ	air density

Subscripts:

a	air at reference level
b	leaf boundary (subscript of r)
al	aerodynamic layer above canopy
a2	aerodynamic layer within canopy
ah	aerodynamic; specific for heat
c	canopy or air stream within canopy
g	bare ground, skin layer in VB95
h	heat (subscript of Ψ)
h1, h2	soil layer 1, 2; heat (subscript of r)
l	canopy leaves
q1	soil layer 1; moisture (subscript of r)
s	stomatal, crop (subscript of r)
sur	effective surface (subscript of T)
0h	aerodynamic roughness for heat (subscript of z)
0m	aerodynamic roughness for momentum (subscript of z)
1,2...	soil layer

REFERENCES

Beljaars, A. C. M. and Holtslag, A. A. M. 1991 Flux parameterizations over land surface for atmospheric models. *J. Appl. Meteorol.*, **30**, 327–341

Bhumralkar, C. M. 1975 Numerical experiments on the computation of ground surface temperature in an atmospheric general circulation model. *J. Appl. Meteorol.*, **14**, 1246–1258

Blondin, C. 1991 Parameterization of land-surface processes in numerical weather prediction. Pp. 31–54 in *Land surface evaporation: measurements and parameterization*. Eds T. J. Schmugge and J. C. André. Springer

Blyth, E. M. and Dolman, A. J. 1995 The roughness length for heat of sparse vegetation. *J. Appl. Meteorol.*, **34**, 583–585

Bolle, H. J. and Streckenbach, B. 1993 The Echival field experiment in a desertification threatened area—Final Report. Free University of Berlin, Germany

Bolle, H. J., Andre, J. C., Arrue, J. L., Barth, H. K., Bessemoulin, P., Brasa, A., de Bruin, H. A. R., Cruces, J., Dugdale, G., Engman, E. T., Evans, D. L., Fantechi, R., Fiedler, F., van de Griend, A., Imeson, A. C., Jochum, A., Kabat, P., Kratzsch, T., Lagouarde, J.-P., Langer, I., Llamas, R., Lopez-Baeza, E., Melia Miralles, J., Muniosguren, L. S., Nerry, F., Noilhan, J., Oliver, H. R., Roth, R., Saatchi, S. S., Sanchez Diaz, J., de Santa Olalla, M., Shuttleworth, W. J., Sogaard, H., Stricker, H., Thornes, J., Vauclin, M. and Wickland, D. 1993 EFEDA: European field experiment in a desertification threatened area. *Ann. Geophysicae*, **11**, 173–189

Braud, I., Noilhan, J., Bessemoulin, P. and Mascart, P. 1993 Bare ground surface heat and water exchanges under dry conditions: observations and parameterization. *Boundary-Layer Meteorol.*, **66**, 173–200

Choudhury, B. J. and Monteith, J. L. 1988 A four-layer model for the heat budget of homogeneous land surfaces. *Q. J. R. Meteorol. Soc.*, **114**, 373–398

Clapp, R. B. and Hornberger, G. M. 1978 Empirical equations for some hydraulic properties. *Water Resources Res.*, **14**, 601–604

Deardorff, J. W. 1978 Efficient prediction of ground surface temperature and moisture, with inclusion of a layer of vegetation. *J. Geophys. Res.*, **83**, 1889–1903

Dickinson, R. E., Henderson-Sellers, A., Kennedy, P. J. and Wilson, M. F. 1986 'Biosphere–Atmosphere Transfer Scheme (BATS) for the NCAR Community Climate Model'. NCAR Technical Note NCAR/TN-275+STR

Dolman, A. J. and Wallace, J. S. 1991 Lagrangian and K-theory approaches in modelling evaporation from sparse canopies. *Q. J. R. Meteorol. Soc.*, **117**, 1325–1340

Droogers, P., van Abeele, G. D., Cobbaert, J., Kim, C. P., Rösslerova, R., Soet, M. and Stricker, J. N. M. 1993 'Basic data sets description and preliminary results of EFEDA-Spain'. Dept. of Water Resources, Wageningen Agricultural University, The Netherlands

Garratt, J. R. 1992 *The atmospheric boundary layer*. University Press, Cambridge, UK

Garratt, J. R. and Hicks, B. B. 1973 Momentum, heat and water vapour transfer to and from natural and artificial surfaces. *Q. J. R. Meteorol. Soc.*, **99**, 680–687

Jacobs, C. M. J. 1994 'Direct impact of atmospheric CO_2 enrichment on regional transpiration'. Wageningen Agricultural University, The Netherlands

Keijman, J. Q. 1974 The estimation of the energy balance of a lake from simple weather data. *Boundary-Layer Meteorol.*, **7**, 399–407

Kondo, J., Saigusa, N. and Sato, T. 1990 A parameterization of evaporation from bare soil surfaces. *J. Appl. Meteorol.*, **29,** 385–389

Kustas, W. P., Choudhury, B. J., Moran, M. S., Reginato, R. J., Jackson, R. D., Gay, L. W. and Weaver, H. L. 1989 Determination of sensible heat flux over sparse canopy using thermal infrared data. *Agric. Forest. Meteorol.*, **44,** 197–216

Louis, J.-F. 1979 A parametric model of vertical eddy fluxes in the atmosphere. *Boundary-Layer Meteorol.*, **17,** 187–202

McMillen, R. T. 1988 An eddy-correlation technique with extended applicability to non-simple terrain. *Boundary-Layer Meteorol.*, **43,** 231–245

Menenti, M., Bastiaanssen, W. G. M. and van Eick, D. 1989 Determination of surface hemispherical reflectance with Thematic Mapper data. *Remote Sensing Environ.*, **28,** 327–337

Milly, P. C. D. and Dunne, K. A. 1994 Sensitivity of the global water cycle to the water-holding capacity of land. *J. Climate*, **7,** 506–526

Monteith, J. L. 1965 Evaporation and the environment. *Symp. Soc. Exp. Biol.*, **19,** 205–234

1995 A reinterpretation of stomatal responses to humidity. *Plant, Cell and Environment*, in press

Moore, C. J. 1986 Frequency response corrections for eddy correlation systems. *Boundary-Layer Meteorol.*, **37,** 17–35

Noilhan, J. and Planton, S. 1989 A simple parameterization of land surface processes for meteorological models. *Mon. Weather Rev.*, **117,** 536–549

Raupach, M. R. 1992 Drag and drag partition on rough surfaces. *Boundary-Layer Meteorol.*, **60,** 375–395

Sellers, P. J., Mintz, Y., Sud, Y. C. and Dalcher, A. 1986 A simple biosphere model (SiB) for use within general circulation models. *J. Atmos. Sci.*, **43,** 505–531

Shaw, R. H. and Perreira, A. R. 1982 Aerodynamic roughness of a plant canopy: a numerical experiment. *Agric. Meteorol.*, **26,** 51–65

Shuttleworth, W. J. and Gurney, R. J. 1990 The theoretical relationship between foliage temperature and canopy resistance in sparse crops. *Q. J. R. Meteorol. Soc.*, **116,** 497–519

Shuttleworth, W. J. and Wallace, J. S. 1985 Evaporation from sparse crops—an energy combination theory. *Q. J. R. Meteorol. Soc.*, **111,** 839–855

Thom, A. S. 1972 Momentum, mass and heat exchange of vegetation. *Q. J. R. Meteorol. Soc.*, **98,** 124–134

Van den Hurk, B. J. J. M. and McNaughton, K. G. 1995 Implementation of near-field dispersion in a simple two-layer surface resistance model. *J. Hydrol.*, **166,** 293–311

Verhoef, A., van den Hurk, B. J. J. M., Jacobs, A. F. G. and Heusinkveld, B. G. 1995 Thermal soil properties for a vineyard (EFEDA-I) and a savanna (HAPEX-Sahel) site. *Agric. Forest. Meteorol.*, in press

Viterbo, P. and Beljaars, A. C. M. 1995 'An improved land surface parameterization scheme in the ECMWF model and its validation'. Technical Report TR-75, ECMWF, Reading, UK

Webb, E. K., Pearman, G. I. and Leuning, R. 1980 Correction of flux measurements for density effects due to heat and water vapour transfer. *Q. J. R. Meteorol. Soc.*, **106,** 85–100